

Progress in Physical Geography

<http://ppg.sagepub.com>

HRSC-A data: a new high-resolution data set with multipurpose applications in physical geography

J.-C. Otto, K. Kleinod, O. König, M. Krautblatter, M. Nyenhuis, I. Roer, M. Schneider, B. Schreiner and R. Dikau

Progress in Physical Geography 2007; 31; 179

DOI: 10.1177/0309133307076479

The online version of this article can be found at:
<http://ppg.sagepub.com/cgi/content/abstract/31/2/179>

Published by:

 SAGE Publications

<http://www.sagepublications.com>

Additional services and information for *Progress in Physical Geography* can be found at:

Email Alerts: <http://ppg.sagepub.com/cgi/alerts>

Subscriptions: <http://ppg.sagepub.com/subscriptions>

Reprints: <http://www.sagepub.com/journalsReprints.nav>

Permissions: <http://www.sagepub.com/journalsPermissions.nav>

Citations (this article cites 59 articles hosted on the SAGE Journals Online and HighWire Press platforms):
<http://ppg.sagepub.com/cgi/content/refs/31/2/179>



HRSC-A data: a new high-resolution data set with multipurpose applications in physical geography

J.-C. Otto,^{1*} K. Kleinod,¹ O. König,¹
M. Krautblatter,¹ M. Nyenhuis,¹ I. Roer,²
M. Schneider,³ B. Schreiner⁴ and R. Dikau¹

¹Department of Geography, University of Bonn, Meckenheimer Allee 166, 53115 Bonn, Germany

²Swiss Federal Institute for Forest, Snow and Landscape Research (WSL), Zürcherstrasse 111, 8903 Birmensdorf, Switzerland

³Department of Computer Science II, University of Bonn, Römerstraße 164, 53117 Bonn, Germany

⁴Department of Geology, University of Berlin (FU), Malteserstraße 74-100, 12249 Berlin, Germany

Abstract: The analysis and interpretation of remote sensing data facilitates investigation of land surface complexity on large spatial scales. We introduce here a geometrically high-resolution data set provided by the airborne High Resolution Stereo Camera (HRSC-A). The sensor records digital multispectral and panchromatic stereo bands from which a very high-resolution ground elevation model can be produced. After introducing the basic principles of the HRSC technique and data, applications of HRSC data within the multidisciplinary Research Training Group 437 are presented. Applications include geomorphologic mapping, geomorphometric analysis, mapping of surficial grain-size distribution, rock glacier kinematic analysis, vegetation monitoring and three-dimensional landform visualization. A final evaluation of the HRSC data based on three years of multipurpose usage concludes this presentation. A combination of image and elevation data opens up various possibilities for visualization and three-dimensional analysis of the land surface, especially in geomorphology. Additionally, the multispectral imagery of the HRSC data has potential for land cover mapping and vegetation monitoring. We consider HRSC data a valuable source of high-resolution terrain information with high applicability in physical geography and earth system science.

Key words: geomorphological mapping, geomorphometry, High Resolution Stereo Camera, HRSC-A, rock glacier kinematics, vegetation monitoring.

*Author for correspondence. Email: j.otto@giub.uni-bonn.de

I Introduction

The high complexity of the land surface represents a challenge to researchers in physical geography and earth system sciences. This complexity is expressed by a highly differentiated spatial arrangement of objects and a complex interaction between its components. The analysis and interpretation of remote sensing data facilitates investigation of land surface complexity on large spatial scales. The geometrical, spectral and temporal resolution of this data determines what level of complexity we can observe. Remote sensing techniques and data interpretation methods have constantly evolved for several decades, increasing the spatial, temporal and spectral resolution of the information and providing a continuous (complete) spatial coverage of the planet's land surface. Generally, remote sensing data are useful for area-wide monitoring and for monitoring of areas that are difficult to access and that have a global dimension. Increasing spatial and temporal resolution and decreasing costs make these data increasingly useful for physical geography.

We introduce in this paper a geometrically high-resolution data set provided by the airborne High Resolution Stereo Camera (HRSC-A). The HRSC-A system is an airborne digital pushbroom (linear array CCD) scanner. From one single campaign the user receives multispectral data and can derive very precise elevation information. High-resolution digital elevation data comparable to the HRSC technique, with a geometrical resolution between 0.1 m and 1 m, can be obtained by airborne laser scanning (LIDAR), satellite-based radar (InSAR) or by stereoscopic imagery techniques. Comparable multispectral data is obtained by high-resolution satellite sensors (Ikonos, QuickBird) or by multispectral airborne imagery sensors (eg, ADS40, UltraCam-D, DMC).

High geometrical resolution data is applied in a broad range of subjects in physical geography. Digital elevation data derived from airborne LIDAR is increasingly used in geomorphology. Glacier monitoring (Kennett and Eiken 1997; Baltsavias *et al.*, 2001; Geist

et al., 2003; Tamburini *et al.*, 2005), reconstruction of relict glaciation patterns (Kovanen and Slaymaker, 2004), analysis of debris flow depositional patterns (Staley *et al.*, 2006), the characterization of landslide morphology and activity (McKean and Roering, 2004; Glenn *et al.*, 2006; Staley *et al.*, 2006) are some examples of LIDAR data applications in geomorphology. Hydrological research applies LIDAR data to analyse erosion and deposition of river systems (Lane *et al.*, 2003) and for hydrologic modelling (French, 2003). In biogeography LIDAR is used for vegetation structure detection (Ni-Meister, 2005; Kimes *et al.*, 2006). InSAR data is applied in glacial and periglacial hazard assessment (Kääb *et al.*, 2005), detection of mountain periglacial creep (Strozzi *et al.*, 2004) and slope movement studies (Squarzoni *et al.*, 2003; Metternicht *et al.*, 2005; Saroli *et al.*, 2005; Singh *et al.*, 2005). An overview of digital terrain models (DTM) derived by satellite stereo images with, for example, QuickBird, Ikonos or EROS is given in Toutin (2004).

Spectral images of QuickBird or Ikonos satellites and airborne sensors like ADS40 are increasingly used for environmental investigations. Research focuses mainly on monitoring vegetation or land use in different regions and in varying vegetation types. For instance, vegetation mapping in topographically complex hills (Zhang *et al.*, 2006a), estimation of vegetation fraction (Chen and Chen, 2005) and density measurements of forest trees (Keramitsoglou *et al.*, 2005) become possible with highly geometrical and spectral resolved remote sensing data. Many habitat mappings and land use classifications were realized using QuickBird or Ikonos data (see, for example, Bock *et al.*, 2005; also with HRSC, Kobler *et al.*, 2006). For agricultural applications, especially precision farming, the new sensors are promising tools, eg, for the detection of site-specific damage in cultivation systems (Voß, 2004), for biomass and yield estimation (Yang *et al.*, 2004; Heinzl *et al.*, 2005) or for predicting nitrogen in leaves (Zhang *et al.*, 2006b). Hydrologic and geomorphologic investigations also use the new sensors, eg, for

detecting floods (Glaßer and Reinartz, 2005), measuring river discharges (Xu *et al.*, 2004), monitor shrinking processes and groundwater processes in discontinuous permafrost (Yoshikawa and Hinzman, 2003) or detecting landslides (eg, Delacourt *et al.*, 2004; Metternicht *et al.*, 2005; Nichol and Wong, 2005) and slope failures (Kawamura *et al.*, 2003). Among others, snow and ice monitoring is performed with support by Ikonos images, eg, in order to detect snow cover variation (Budkewitsch *et al.*, 2004) or to analyse rock/ice avalanches (Huggel *et al.*, 2005).

Test flights with the ADS40 produced promising results for the application of the airborne digital camera in future environmental projects (Börner and Reulke, 2001; Cramer, 2005).

The data and applications presented here are from the work of the Research Training Group (RTG) 437 – ‘Landform – a structured and variable boundary layer’, which is a multi-disciplinary graduation program funded by the German Research Foundation (DFG) (<http://www.giub.uni-bonn.de/grk/>). Landform as the boundary surface between different components of the earth system is investigated in this programme within a range of disciplines ranging from geoscience (geomorphology, hydrology, climatology, geodynamics, meteorology, pedology) to biology, mathematics, computer science and remote sensing. The HRSC data is applied within the Alpine cluster of the RTG 437 and covers a 120 km² large area of high Alpine relief in southern Switzerland (Turtmann valley, Valais, Swiss Alps). We introduce here the basic principles of this data type and give examples of applications and visualizations of these data within the scope of the RTG 437 research. Applications include geomorphologic mapping, geomorphometric analysis, mapping of surficial grain-size distribution, rock glacier kinematics analysis, vegetation monitoring and 3D landform visualization. A final discussion of our evaluations of the HRSC data based on three years of multipurpose usage concludes this presentation. We consider the HRSC data a valuable source of high-resolution terrain information with high applicability in physical geography and earth system science.

II The HRSC-A camera and data set

The HRSC was originally developed for the mission ‘Mars Express’ by the German Aerospace Centre (DLR). First airborne experiments on Earth with HRSC-A (A = airborne) showed good results in mapping and in photogrammetry. For this reason, two additional airborne cameras (HRSC-AX 150, HRSC-AXW 47) were developed in 2000 (Neukum, 2001).

The HRSC-A sensor (Table 1) is a multi-spectral and stereo scanner containing nine bands: one blue band, one green band, one red band (tending to near infrared), one near infrared band and five panchromatic bands covering the green and red spectrum. It is a pushbroom scanner consisting of CCD sensors in nine lines. The sensors scan line by line (nine lines at a time) along the flight path (Figure 1). Each CCD line scans another band, each with another viewing angle. The geometrical resolution depends on the flying altitude and starts at 10 cm upwards.

In September 2001 a flight campaign covering the entire Turtmann valley was successfully completed after scanning 13 overlapping parallel tracks from a mean flight altitude of 6000 m (3000–4000 m over ground) using the HRSC-A system. Limited by the lateral field of view (FOV) of the sensors (Table 1), several parallel tracks had to be recorded and mosaiced for each colour and stereo band separately during on-ground processing.

After data processing at DLR including combined determination of position and attitude, geometric correction of image data, image matching, DTM generation, orthoimage generation and mosaicing (Hauber *et al.*, 2000; Scholten *et al.*, 2002), we received a large data set of several Gb consisting of multi-spectral, stereo data as well as a digital terrain model that includes vegetation. Image and DTM data are referenced to the standard Swiss map projection (CHI903). Image data have a radiometric resolution of 8 bits, while the terrain model is coded in 16 bits resolving a height difference of 10 cm. The spatial resolution is 50 cm and 1 m for image data and DTM, respectively. Multispectral data tend

Table 1 Technical data on the HRSC sensors

	HRSC-A	HRSC-AX150	HRSC-AX047
Focal length [mm]	175	151	47
Numbers of CCD lines	9	9	5
Numbers of sensors per line	5184	12.000	12.000
Sensor size [μm]	7	6.5	6.5
Radiometric resolution[bit]	8	12	12
Multispectral viewing angle [$^{\circ}$]	15.9 (R) 3.3 (B) -3.3 (G) -15.9 (nIR)		
Stereo viewing angle [$^{\circ}$]	± 18.9 ± 12.8 0	± 20.5 ± 12	± 14.4
Field of view [$^{\circ}$]	± 11.8	± 29.1	± 79.4
Flight altitude for 20 cm geometrical resolution [m]	5000	4700	1500
Spectral resolution [nm]			
Blue	395–485	450–510	–
Green	485–575	530–570	475–575
Red	730–770	635–685	570–680
Near infrared	925–1015	770–810	–
Nadir (panchromatic)	585–765	520–760	515–750
Stereo forward/backward (panchromatic)	585–765	520–760	515–750
Photometry forward/backward (panchromatic)	585–765	520–760	–
Maximum line frequency per band [Lines/s]	450	1640	1640
Platform	stabilized Zeiss T-AS-Plattform		
Data recording	SONY high speed data recorder		
Weights: camera [kg]	~32	~70	~70
adapter [kg]	~40	~40	~40

to be slightly blurred in the flight direction due to their smaller filter bandwidth (see Table 1) compared to the more panchromatic filters of the stereo bands. This results in longer exposure times. Nevertheless, sharpening can be achieved by using HSI transformation with the very sharp Nadir band as the intensity component.

III Study area

The Turtmann valley is an Alpine catchment located in the southern mountain range of the Pennine Alps between the Matter valley and the Anniviers valley in Switzerland (Figure 2).

The main stream of the valley, a tributary of the Rhone River, drains a 110 km² catchment at altitudes between 620 m and 4200 m a.s.l. The Turtmann valley is a high Alpine valley with a typical glacial relief covered by paraglacial and periglacial landforms. The valley is 20 km long and the main glacial trough is orientated from south to north. The trough is up to 300 m wide and there are 15 hanging valleys to the west and east. Ground levels of the hanging valleys rise from 2300 m to 2600 m a.s.l. In addition to small glaciers in some of the hanging valleys, the Turtmann and Brunegg Glaciers at the valley head cover

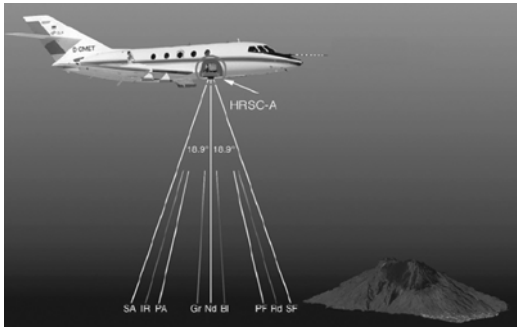


Figure 1 HRSC-A imaging principle
Source: Wewel *et al.* (2000).

approximately 14% of the valley surface. The hanging valleys are characterized by more than 80 recent and relict rock glaciers. Lithologies include palaeozoic schists and gneisses and mesozoic dolomites, limestones, and marbles of the penninic nappe Siviez-Mischabel. The inner Alpine location of the

Turtmann valley is characterized by continental climatic conditions. Mean annual air temperatures are between 8.5°C in the Rhone valley (Sion) and 3.8°C at 1825 m (Evolène). Mean annual precipitation is about 500–600 mm (surrounding stations) (data from www.meteoschweiz.ch).

IV Review of application of HRSC data in physical geography

1 Terrestrial application of HRSC data in physical geography

Terrestrial commercial application of HRSC data includes disaster management, hydrology, agriculture, forestry, coal mining, urban mapping and telecom. Experiments on active volcanoes and on glaciers have demonstrated the potential of the camera system for mapping rugged terrain for example in high Alpine environments (Gwinner *et al.*, 1999; Hauber *et al.*, 2000). There have been only few research projects applying the terrestrial HRSC data so far. Most of them investigated vegetation by



Figure 2 View across the glacial trough of Turtmann Valley into the western hanging valleys

mapping biotopes or classifying land cover at small scales. For instance, Ehlers *et al.* (2003) developed an automated analysis of HRSC data for biotope mapping in northern Germany. Their hierarchical classification approach combined stepwise multispectral bands, vegetation indices (NDVI), texture measures and the DTM of the HRSC to separate more than 20 biotope classes. Providing very high geometrical resolution and position accuracy and with four multispectral bands, HRSC-AX data delivered even better biotope mapping results than the analysis of aerial photographs. According to Ehlers *et al.* (2003), the red band, near infrared band and particularly the NDVI $((nIR + R)/(nIR - R))$ were useful to distinguish vegetation from non-vegetation and to differentiate vegetation types. Texture measures like variance filters were calculated to separate smooth (eg, grassland) and rough vegetation (eg, shrubs, reeds). The DTM improved the division of high-growing vegetation like trees and short vegetation like grassland. Besides, landform parameters derived from the DTM as additional information about the abiotic environment can improve vegetation mapping. Leser (2003) and Bock *et al.* (2005) succeeded in classifying habitats semi-automatically at a local scale. Bock *et al.* (2005) first segmented the HRSC data and then developed the habitat classification method. As assessment, classifying and documenting vegetation with digital data is united in one procedure, vegetation mapping is more time-efficient and less error-prone than with aerial photographs. Moreover, low repeating rates and the transferability of classification methods to multitemporal data permit monitoring of vegetation using time series. Lehmann *et al.* (1998) fused data of the very high geometrical resolution HRSC with the very high spectral resolution HyMap sensor to extract trees in urban areas automatically. Both spectral and textural information led to a precise classification of urban vegetation.

2 Extraterrestrial application of HRSC data

The nominal mission of the Mars Express was fulfilled on 30 November 2005 after 2418

orbits round Mars. During highly elliptical polar orbits, the HRSC camera operated most of the time only near the periapsis, when it approached c. 250 km above the Mars surface. Thus, a resolution of 20 metres/pixel was attained for 28% of Mars's surface while 41% were covered with a resolution of 30 metres/pixel (Hauber and Neukum, 2006). A number of new research findings were made possible by higher-resolution, improved spectral information and larger contiguous coverage of the HRSC data set. Above all, refined dating possibilities, based on a high-resolution survey of impact crater size and frequency, brought a number of new research applications into being and revitalized existing ones (Neukum *et al.*, 2004). The disciplines that profited profoundly from the HRSC data include geology, mineralogy, hydrology and climatology, as well as volcanic (peri-)glacial and fluvial geomorphology.

The extraordinary huge volcanic landforms were the first that were observed during the approach of the Mariner 9 cameras to Mars in 1971. Ever since, much attention has been paid to understanding and dating the volcanic history of Mars. The better dating possibilities of the HRSC data set and a resolution suitable for the mapping of lava flows and pyroclastic deposits helped to establish a more accurate chronology of the volcanic activity on Mars (Neukum *et al.*, 2004). Prior missions detected glacial and periglacial landforms, mostly in the latitude belts 30–70° in both hemispheres. The HRSC data uncovered a number of previously unknown occurrences in all latitudes including some of very limited spatial extent in extraordinary topographic settings such as volcano craters (Neukum *et al.*, 2004; Hauber *et al.*, 2005; Head *et al.*, 2005; Helbert *et al.*, 2005; Murray *et al.*, 2005). Fluvial and lacustrine geomorphologic features witness the presence of water and have, therefore, always received special attention. Fluvial channels can be tracked for more than 100 km in length in the HRSC data (Hauber *et al.*, 2005; Jaumann *et al.*, 2005; Hauber and Neukum,

2006). The study of long-term hydrological fluctuations profited much from the improved dating methods and a spatial resolution that supports the detection of near-surface water and ice (Helbert *et al.*, 2005; Ivanov *et al.*, 2005; Reiss *et al.*, 2005). Enhanced understanding of the phases of fluvial activity now suggests a series of environmental changes rather than a unique period of enhanced fluvial activity. More evidence for the existence and importance of water is provided by mineralogical deposits. Even if hydrated alteration minerals (hydrated sulphates and phyllosilicates) were detected mainly with the aid of the OMEGA spectrometer of the Mars Express Mission (Arvidson *et al.*, 2005; Gendrin *et al.*, 2005; Poulet *et al.*, 2005), HRSC imagery can decipher the dip direction and angle of dip of rock layers in complex geological settings and thus contribute to the geological understanding and mapping of Mars (Basilevsky *et al.*, 2005; Korteniemi *et al.*, 2005). The high scanning frequency of the same ground position (four days) and the timelag between the forward-looking stereo sensor and other bands (several minutes) makes HRSC data even attractive for the observation of rapidly changing environmental systems. Thus, it was applied to the analysis of climatologic processes on Mars and in some case even yielded information on the speed and direction of wind systems (Hauber and Neukum, 2006).

V Applications of the HRSC data within RTG 437

1 The use of HRSC data in geomorphological mapping and geomorphometric land surface analysis

The complexity of the land surface originates from its three-dimensional spatial character and its four-dimensional time-dependent nature (Lane *et al.*, 1997). Mapping of geomorphological landforms is the traditional technique to decompose land surface complexity into structural patterns, landforms and landform elements, often providing the database for further geomorphological research.

The accuracy of digital landform mapping, whether transferred from previously acquired field data, or genuinely digitized on screen, depends on the resolution of the topographic base data and the visual perception of the virtual land surface morphology on a two-dimensional screen. In RTG 437, large-scale geomorphologic mapping and geomorphometric land surface analysis are applied in several subprojects. Rasemann (2004; see also Rasemann *et al.*, 2004) characterized Alpine landforms at different spatial scales taking a geomorphometric approach. Nyenhuis (2005) mapped rock glaciers in order to model the permafrost distribution in the Turtmann valley. Otto and Dikau (2004) created a qualitative sediment budget model of the valley based on a detailed geomorphological map at a scale of 1:25,000. Otto (2007) mapped the sediment storage landforms in order to assess the role of storage within the sediment budget of the valley. Figure 3 depicts different visualization techniques for geomorphological mapping using the HRSC data set of the Turtmann valley. High-resolution aerial photographs are the ordinary basis used for mapping. However, a simple, two-dimensional bird's-eye-view visualization of imagery data restricts the perception of landforms to strong contrasts and large objects. Derivatives of elevation can be used to accentuate morphology changes and break lines in the land surface (Smith and Clark, 2005). For example, relief-shading (Figure 3a) is commonly used for visualizations; however, it is prone to biasing due to the variable azimuth of the lighting source (Smith and Clark, 2005). A simple slope map (Figure 3b) does not contain such biasing and depicts land surface changes very clearly as well, at least in regions of strong slope variability. By combining imagery and elevation data (Figure 3c), a three-dimensional visualization further enhances the recognition of landforms, as our natural three-dimensional perception is simulated on the screen. The high geometrical resolution of the elevation data enables the recognition of small

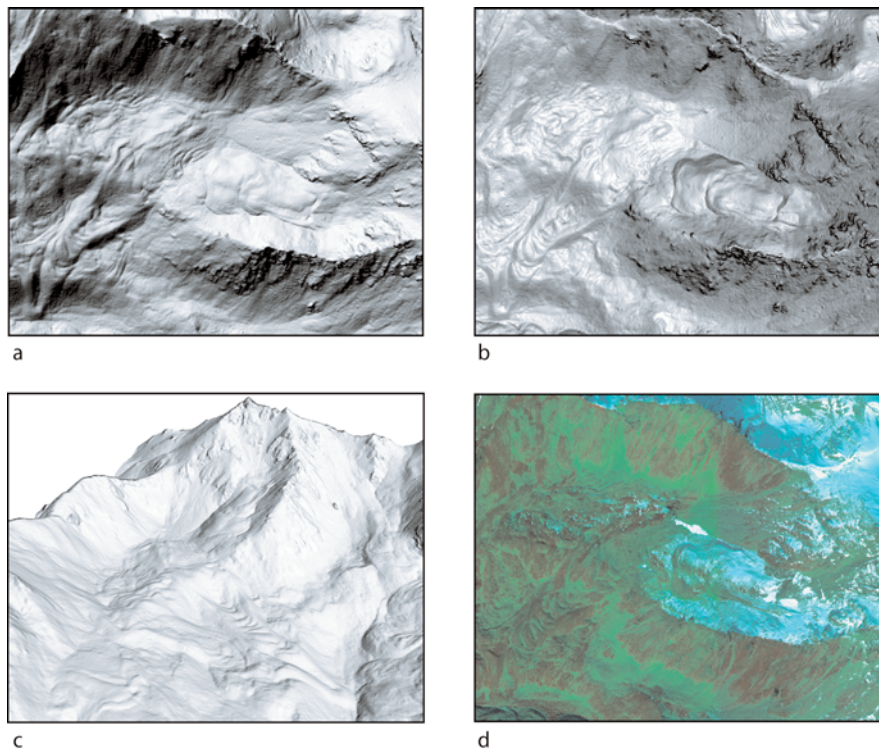


Figure 3 Visualization of HRSC data for landform mapping purposes. The scene depicts the northern part of the Hungerlitaelli hanging valley, showing active and relict rock glaciers, talus slopes and block slopes. (a) Relief-shaded DTM. (b) Slope map. (c) Relief-shaded DTM including altitude information (3D scene). (d) Aerial photograph of the same scene. The colour version (see online publication) of this image reveals the shift of the red band towards near infrared in the HRSC-A data that enhances the vegetation reflection

scale landforms or landform structures, often superimposed on larger ones. Small solifluction lobes forming on non-vegetated slopes may not be clearly distinguishable when the surrounding slope is of the same material. A visualization using elevation data, though, would single out the form, for example by the rise of the lobe front above the talus slope surface. Additionally, multispectral image data enables the distinction of vegetated and non-vegetated surfaces, thus revealing process activity on certain landforms, such as talus slopes (Figure 3d).

The parameterization and characterization of the land surface structure of Alpine regions

represents a key issue for high mountain geomorphology and geomorphometry. In general, geomorphometric analysis of the land surface aims at providing quantitative data on geometrical and topological characteristics of the land surface (Pike and Dikau, 1995; Schmidt and Dikau, 1999). Geomorphometric parameters are derived by analysing DTM data or direct measure of simple parameters such as altitude, slope or aspect in the field.

To analyse geomorphometric structure of single microscale landforms, DTMs with appropriate geometrical resolution and accuracy are required (Rasemann, 2004; Rasemann *et al.*, 2004). The HRSC DTM

provides a good basis for the analysis of microscale geomorphological forms such as rock glaciers on a regional scale. Nevertheless, the resolution of the DTM has to be adjusted to an appropriate level of detail. In order to quantify curvature and form elements at the surface of rock glaciers, Rasemann (2004) developed a variable Gaussian filter to resample and smooth the DTM. A comparison of curvature classifications based on the original, non-smoothed DTM with smoothed data proved the necessity of object adapted DTM resolution (Rasemann, 2004).

To illustrate the potential of the HRSC technology for land surface structure visualization and analysis, a relict rock glacier and its surrounding area are shown in Figure 4. After smoothing of the DTM with a Gaussian filter, nine different landform elements, each characterized by homogenous curvature, have been classified according to the geomorphographic land surface model developed by Dikau (1989). The rock glacier can be differentiated from other neighbouring landforms such as talus slopes or moraine ridges by its typical surface structure. The surface structure of the rock glacier is characterized by regularly distributed ridges (landform elements X/X) and furrows (landform elements V/V). These structures are associated

with the flow field of the rock glacier and are orientated in accordance with the internal stress field (Haeberli, 1985; Barsch, 1996). Longitudinal and transverse wall structures indicate zones of former extending and compressing flow. Pronounced collapse structures in the centre of the rock glacier denote the disappearance of permafrost ice and the relict age of the landform.

The HRSC data proved to be a valuable source of information for detailed geomorphologic mapping and geomorphometric land surface structure analysis at micro to meso scales in this geosystem.

2 Deriving surficial grain-size distribution from HRSC data

An important part of the Alpine sediment cascade is the storage of sediment within the system. Thus a variety of sediment storage types, such as talus cones, moraines and rock glaciers form the landscape. Especially in high mountain geosystems, where wide areas are unvegetated, the surficial grain-size distribution allows inferences about the formative processes. Hence different sediment storage types can be detected by identifying different grain-size patterns.

In a Diploma thesis associated with the RTG 437, the HRSC data was used for a

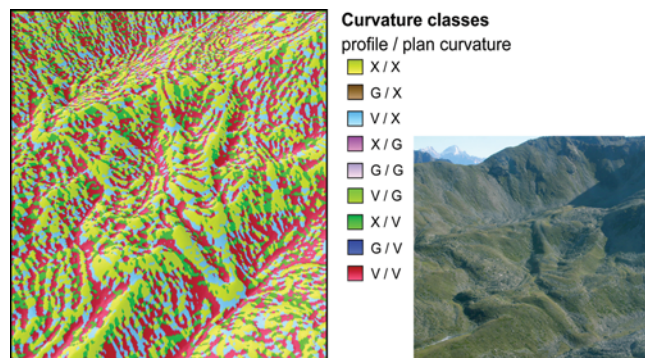


Figure 4 Land surface classification of a hanging valley location. The surface structure of the rock glacier (centre) and surrounding areas indicate surface characteristics typical of this landform. Note the longitudinal and transversal furrows and ridges that indicate the former rock glacier dynamics

straightforward remote sensing approach to determine the grain-size distribution at the surface of different landforms. The Nadir band was especially useful. Texture analysis of the aerial data can provide information about surface roughness and thus grain size. While smaller grain sizes result in a comparatively homogenous texture, bigger rocks cast shadows and lead to a more irregular texture as darker shadows are located next to lighter rocks. One way to quantify the texture is the standard deviation (Haralick *et al.*, 1973). Here we used a moving window of 10×10 pixels, which showed the best results compared to the field data. The real grain sizes of rocks at the surface were determined at 46 test sites in the Turtmann valley. Using a multiple linear regression analysis, the grain sizes were then assigned to the results of the texture analysis. With this method a coefficient of determination (R^2) of 0.78 could be reached (König, 2006). Thus area-wide grain-size information was obtained (Figure 5).

Related to sediment storage types different grain-size patterns have been detected. Talus

sheets and talus cones show a longitudinal sorting in which grain size decreases towards the head wall. This is due mainly to fall sorting and a sieving effect in the lower section (Church *et al.*, 1979). Lateral sorting is also observed on these landforms, a pattern produced by secondary processes on the talus surface such as debris flows, dry debris slides or snow avalanches (Perez, 1998). Rock glaciers in contrast show a complete different pattern in the Turtmann basin. Their surface is very coarse with mean grain sizes between 0.5 m and 1.1 m. Fine sediment is found only at the front and in very active parts. Figure 5 displays a transition zone between a sorted talus sheet and a blocky rock glacier complex. Other sediment storage types such as moraines or debris cones do not show a typical pattern but can be distinguished by their mean grain size. The detection of different sediment storage types is only one application of area-wide grain-size information. They can further be used for a more detailed description of talus genesis and the processes involved. Permafrost models also could be improved by incorporating grain-size

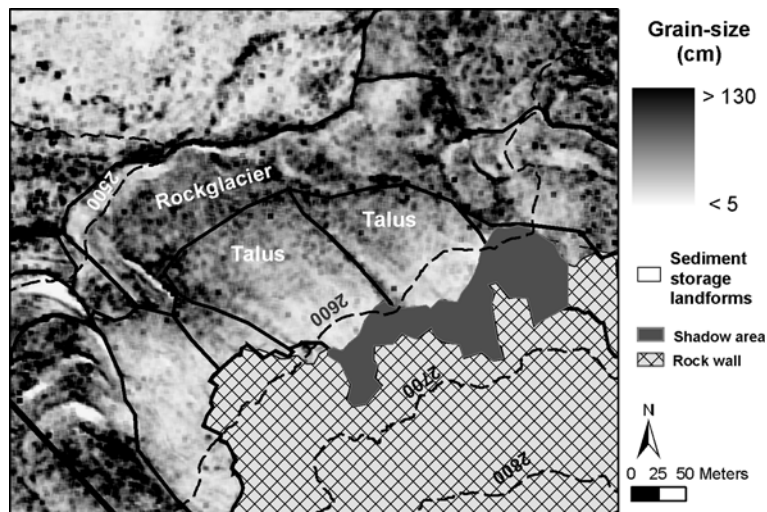


Figure 5 Surface sediment distribution derived from HRSC image analysis on various landforms on a north-facing slope. Note the grain-size increase between talus slopes and rock glacier. The talus cones show a distinct sorting pattern. The rock glacier front is clearly distinguishable by smaller grain sizes

information (Gorbunov *et al.*, 2004; Nyenhuis, 2005). The accuracy and high geometrical resolution of the HRSC data facilitated grain-size estimation in this environment.

3 Rock glacier kinematics using digital photogrammetry on HRSC data

Rock glaciers and their current state of activity are important indicators for the recent or former occurrence of permafrost in high mountain environments. The activity of the creeping mass is commonly described and measured by the application of geodetic surveys (GPS, total station) or by the comparison of multitemporal aerial photographs. Since rock glaciers are often situated in inaccessible terrain, use of remote sensing gives considerable advantages.

To describe rock glacier kinematics, geometrical changes of the landforms are measured; therefore multitemporal data are required. Since rock glacier creep rates of some decimetres per year are expected (Barsch, 1996), a relatively long timespan is needed between the data sets to determine changes at a significant level. For this reason, the HRSC imagery of the year 2001 was combined with aerial photos from the years 1975 and 1993. Hence, the HRSC data set (DTM and orthophoto) was applied for the first time for the measurement of rock glacier movements (Roer *et al.*, 2005a).

A DTM with 10 m spacing and orthophotos with 0.5 m ground resolution were generated from small-scale aerial stereo-photography. The absolute RMS accuracy of the data is roughly estimated to lie within a range of two pixels (ie, here ± 1 m) (Roer *et al.*, 2005a). Regarding the HRSC data, the automated digital photogrammetric processing system delivered a DTM with a horizontal ground resolution of 1 m and multispectral orthoimages with a resolution of 0.5 m. For both data sets, steep terrain or low contrast (due, for example, to snow cover) lower the accuracy of the data. Differences between the two data sets arise both from recording and processing (Roer *et al.*, 2005a).

Quantification of movement was obtained by the tracking of single blocks at the rock glacier surface using the software CIAS (Kääb and Vollmer, 2000) to give the two-dimensional horizontal component of movement. Vertical movements were quantified by the comparison of multitemporal DTMs using a standard GIS. A detailed error assessment is given in Kääb and Vollmer (2000) and in Roer *et al.* (2005a).

In the study presented here, 30 rock glaciers were investigated by the methods described before. One example is given in Figure 6, showing the annual horizontal velocities during 1975–93 and 1993–2001 of one rock glacier in the Turtmann Valley. As expected, most of the rock glaciers showed clear movement rates of several decimetres per year. Furthermore, all actively creeping rock glaciers indicate a distinct increase in their movement rates during the period 1993–2001, in comparison to the period 1975–93 (Figure 6). It is supposed that this acceleration is related to the general increase in air temperature in the Alps and the related increase in ice temperature (Roer *et al.*, 2005b; Kääb *et al.*, 2007).

Owing to possible hazards related to permafrost creep (Kääb *et al.*, 2005) and the reaction of rock glaciers to climatic changes (Roer *et al.*, 2005b; Kääb *et al.*, 2007), future investigations will continue and expand the monitoring of rock glacier kinematics.

4 HRSC potentials for monitoring vegetation

There have been only a few projects concerning the terrestrial application of HRSC data (cf. section IV.1). Most of them investigated vegetation monitoring by mapping biotopes or classifying land cover at small scales.

The HRSC sensor has an enormous potential in vegetation mapping at small scales, particularly the HRSC-AX with its red band introduced for terrestrial observations. Because of the geometrically very high-resolution data, even single objects, eg, trees or shrubs, can be detected (Figure 7). But contour blurring caused by different viewing

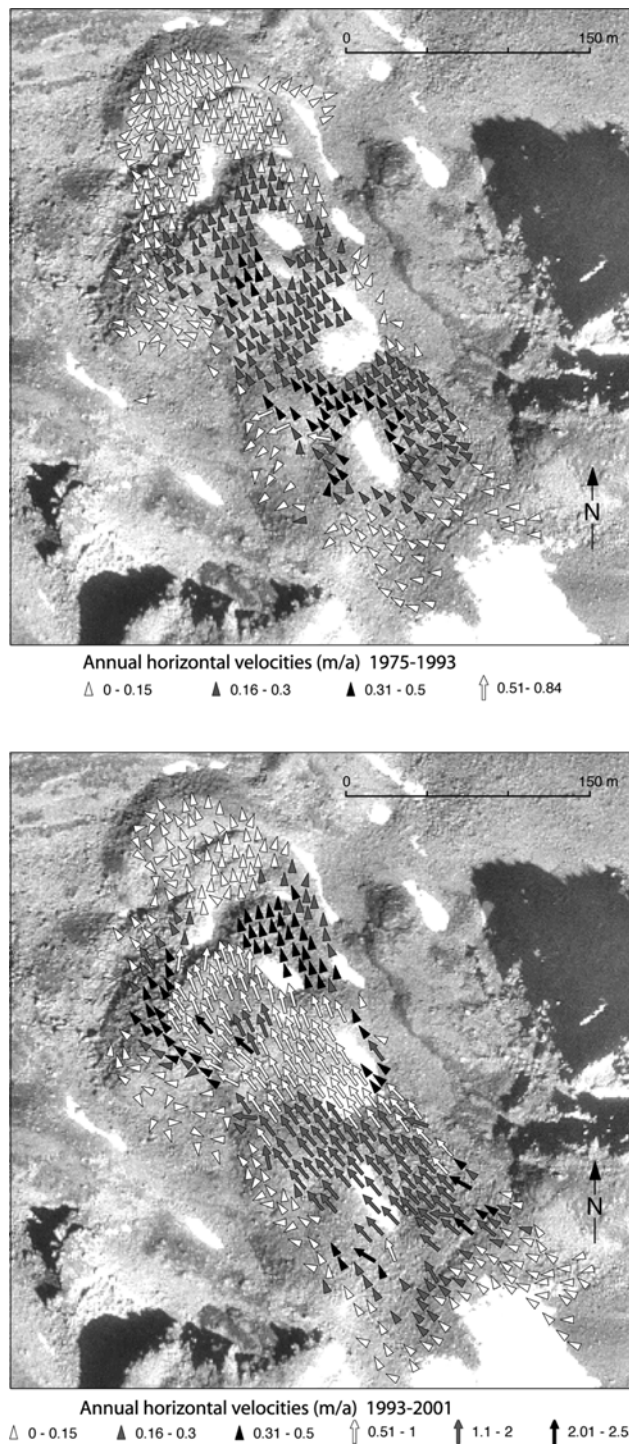


Figure 6 Results of the photogrammetric analyses: annual, horizontal velocities during 1975–93 and 1993–2001 on one rock glacier in the Turtmann Valley, Swiss Alps

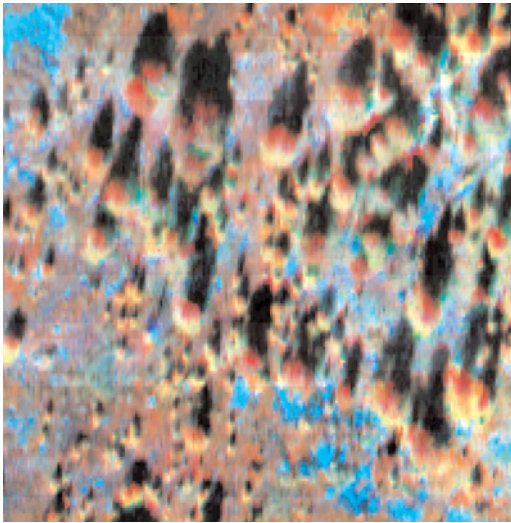


Figure 7 Trees and shrubs in the Turtmann valley, HRSC-A bands 3 (R), 2 (G), 1 (B). Different light effects demonstrate the contour blurring caused by different viewing angles

angles and shadow effects decrease the exact identification in some cases. Of particular importance is the combination of multispectral bands with a digital surface model. Textural measures and DTM derived parameters, for instance, provide high potentials for

detection of small-scaled heterogeneity of vegetation, vegetation patterns, biodiversity measures and their relations to the abiotic environment. Figure 8 shows similar structures in texture derived by the HRSC-A data and a vegetation map of the Turtmann valley created by Hörsch (2003) on the basis of Landsat TM, IRS LISS and colour-infrared aerial photographs. Without going into detail, forests, grassland and debris vegetation can be distinguished approximately from a first visual interpretation. In particular, the structure of forests and shrubs can easily be identified in the variance filter image generated with a 3×3 kernel from the HRSC image. Vegetation research with the HRSC optical data in the Turtmann valley was not carried out as the acquisition date in the year was too late for vegetation monitoring and some regions were already covered by snow (the very light to white parts of the texture image in Figure 8a).

However, the geometrically very high-resolution sensor is recommended for small-area mapping of plant communities or biotopes. HRSC-AX evolved from HRSC-A and is preferable for terrestrial research. In the future, sensors with the same precise ground resolution should provide a better spectral resolution; hyperspectral data will augment spectral differentiation of vegetation types.

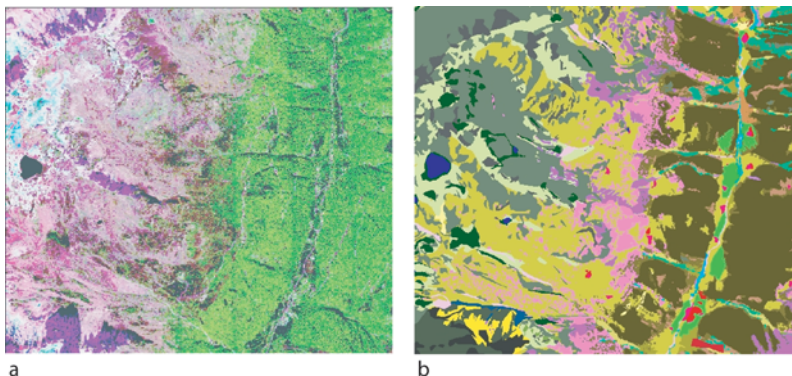


Figure 8 Texture measures and a vegetation map show similar coarse patterns in a small part of the Turtmann Valley. (a) Variance filter of the HRSC-A bands 2 (R), 3 (G), 1 (B). (b) Vegetation map of Hörsch (2003). Dark green = forest; purple = shrubs, light green = alpine grassland; grey = debris and debris vegetation

5 *Three-dimensional visualization of very large DTM data sets*

Efficient interactive visualization of large-textured terrain models is of increasing interest in scientific visualization, virtual reality applications and GIS. What makes it a challenging problem is the sheer size of the raw data sets that easily exceeds the capabilities of current hardware in respect of memory requirements and rendering throughput.

Even with the application of compression techniques, large data sets do not fit completely into the main memory and most of the data must reside on the orders of magnitude slower hard disk. Therefore, the use of suitable caching strategies is indispensable. Although rendering throughput in modern graphic processing units (GPU) has surpassed 100 million triangles per second, large DTMs often contain billions of triangles, far too many to render interactively by brute force. Thus, the graphics rendering load must be controlled by reducing the number of rendered primitives using hierarchical-level-of-detail (HLOD) techniques, which reduce the amount of detail used to render small or distant parts of the visible terrain without sacrificing visual quality. Terrain textures often have an even higher ground resolution than the corresponding DTM. Hence, compression and level of detail (LOD) generation, ie, downsampling to lower resolutions, is just as important here.

In order to allow efficient visualization, the raw data set has to be preprocessed into a representation that is suitable for rendering. In a preprocessing step a HLOD representation of the data is created. This is performed by partitioning geometry as well as textures into equally sized tiles that are associated with the lowest level of the hierarchy. Tiles on higher levels are constructed bottom-up by geometry simplification and texture filtering respectively. Furthermore, state-of-the-art compression techniques are applied to the geometry and texture tiles resulting in high compression ratios; for example, the Turtmann Valley data set was reduced by a

factor of 10 with a guaranteed screen space error of 1 pixel.

The actual rendering is performed by traversing the hierarchy and selecting tiles by considering their visibility and detail. After traversal the selected tiles are sent to the GPU to be rendered. Parallelism between CPU, GPU and the I/O subsystem is exploited in two places during rendering. While traversal is still running, already requested tiles are loaded from the hard disk in parallel. During rendering on the GPU tiles that are likely to be visible in subsequent frames are preselected and cached in main memory in order to accelerate their future retrieval. Using the technique described, it is possible to visualize the Turtmann Valley data set at real-time frame rates. Figure 9 shows a screenshot of the three-dimensional visualization of the HRSC data. It is important to note that the number of tiles to be rendered is generally constant and therefore performance is not limited by the amount of input data, but depends only on the complexity of the visible data and on the available hardware.

A major challenge for future research is the augmentation of the terrain with additional data from various sources, eg, vector data as used in common shape files. There also exist many 3D data sets and models about the earth interior, but less effort has been spent on the realization of combined real-time visualization of three-dimensional volume and terrain data sets.

VI Conclusion

Summarizing all research activities, HRSC is a very useful sensor for geomorphological surface structure mapping, surface sediment detection, landform kinematics analysis, and vegetation mappings on a micro to meso scale, because of its very high geometrical resolution and accuracy combined with four multispectral bands. The combination of image and elevation data is one of the greatest advantages of this data set, opening up various possibilities for visualization and three-dimensional analysis of the land surface. The high repeating rate

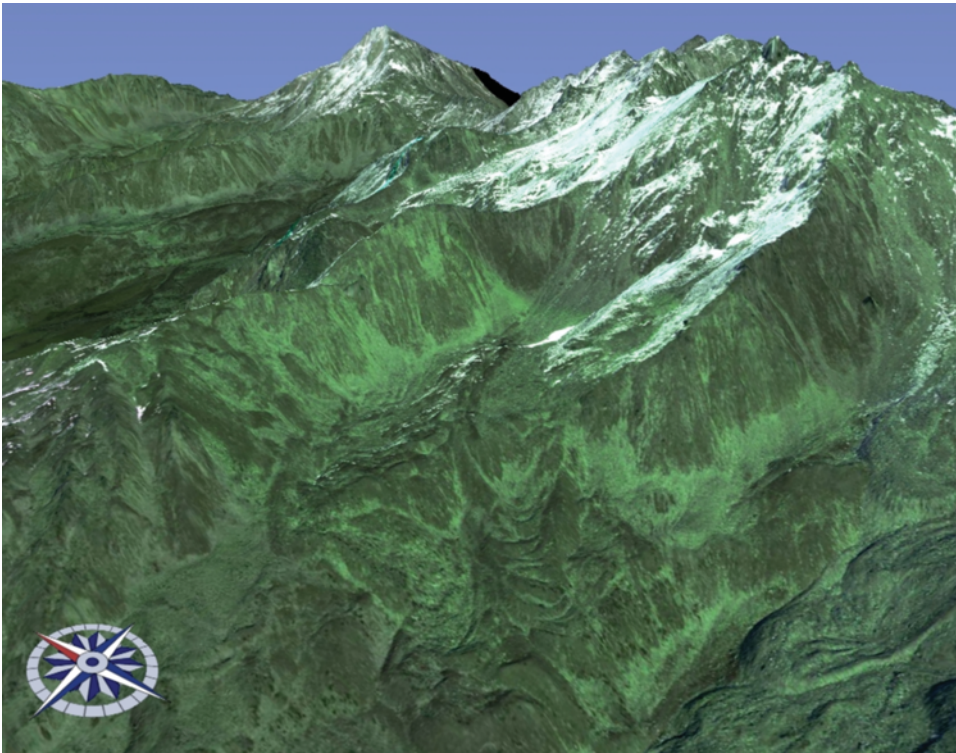


Figure 9 Screenshot of the three-dimensional visualization engine using the Turtmann Valley HRSC data. The colour table of the original image data (see online version for colour image) has been slightly adjusted to represent real colours

compared to field campaigns and the transferability of methods to time series is useful for large-scale multitemporal analysis, eg, monitoring landform movement or vegetation. On the other hand, production costs are very high compared to satellite remote sensing data, but they are similar to airborne multispectral data or LIDAR. Processing of the data, compilation of orthoimages and DTM is done by the DLR and to a certain extent is not reproducible by the user. The HRSC data used in RTG 437 was recorded during the development phase of the HRSC-A camera and unfortunately includes some non-random errors in the DTM data. Errors are represented by regular fabric-like structures along the swath boundaries that rise 10–30 cm above the surface (Rasemann, 2004). Consequently,

geomorphological and geomorphometrical analysis can be biased by these errors. Additionally, the recording date affects the quality and applicability of the image data. Acquisition of the RTG 437 HRSC data took place in late September 2001. The image recording is affected by early autumn snow and the late summer vegetation state. Snow covers large areas above 2900 m (100 m lower in shaded areas). Shaded areas are quite extensive due to a high solar incidence angle. Snow and shadow both influence the generation of the DTM and cause DTM errors in two heavily shaded areas and in some locations with intensive white snow coverage. These errors also need to be considered for DTM analysis. The HRSC-A sensor lacks the red band that, combined with the late acquisition

date of the data, reduced the applicability of the HRSC-A data for vegetation mapping within RTG 437. The HRSC-AX camera is recommended for applications in biogeography. However, because of reduced outline sharpness of the spectral images, edge detection of vegetation and thus tree identification is sometimes difficult. Compared to the HRSC image, digital satellite images provide reflectance information of each spectral band that permit atmospheric correction band by band. For image comparisons in time series (eg, to detect changes) adjustment for different atmospheric conditions is necessary.

In conclusion, the combination of high-resolution air photo and DTM lends the HRSC data to application in multidisciplinary research in geosciences.

Acknowledgements

The RTG 437 program is financed by the German Research Foundation (DFG) which enabled the acquisition of the HRSC data. Funding is gratefully acknowledged by all the members of RTG 437.

References

- Arvidson, R.E., Poulet, F., Bibring, J.-P., Wolff, M., Gendrin, A., Morris, R.V., Freeman, J.J., Langevin, Y., Mangold, N. and Bellucci, G.** 2005: Spectral reflectance and morphologic correlations in eastern Terra Meridiani, Mars. *Science* 307(5715), 1591–94.
- Baltsavias, E.P., Favay, E., Bauder, A., Bösch, H. and Pateraki, M.** 2001: Digital surface modelling by airborne laser scanning and digital photogrammetry for glacier monitoring. *Photogrammetric Record* 17(98), 243–73.
- Barsch, D.** 1996: *Rock glaciers. Indicators for the present and former geocology in high mountain environments.* Berlin: Springer, 331 pp.
- Basilevsky, A.T., Neukum, G., Ivanov, B.A., Werner, S.K., Van Gesselt, S., Head, J.W., Denk, T., Jaumann, R., Hoffmann, H., Hauber, E. and McCord, T.** 2005: Morphology and geological structure of the western part of the Olympus Mons volcano on Mars from the analysis of the Mars Express HRSC imagery. *Solar System Research* 39, 85–101.
- Bock, M., Xofis, P., Mitchley, J., Rossner, G. and Wissen, M.** 2005: Object-oriented methods for habitat mapping at multiple scales – case studies from Northern Germany and Wye Downs, UK. *Journal for Nature Conservation* 13(2–3), 75–89.
- Börner, A. and Reulke, R.** 2001: Results of test flights with the airborne digital sensor ADS40. *Proceedings of SPIE – The International Society for Optical Engineering* 4169, 171–79.
- Budkewitsch, P., Molch, K., Robert, M., Mäher, A., Treitz, P. and Ferguson, M.A.D.** 2004: Temporal snow cover variation and terrain characteristics of Peary caribou habitats in the Canadian Arctic using optical and InSAR data. *International Geoscience and Remote Sensing Symposium (IGARSS)* 7, 4609.
- Chen, Q. and Chen, Y.F.** 2005: A study on estimation of vegetation fraction by using QuickBird imagery. *Forest Research* 18, 375–80.
- Church, M., Stock, R.F. and Ryder, J.M.** 1979: Contemporary sedimentary environments on Baffin Island, N.W.T. Canada: debris slopes accumulations. *Arctic and Alpine Research* 11, 371–402.
- Cramer, M.** 2005: 10 years ifp test site Vaihingen/Enz: an independent performance study. *GeoBit* 8, 35–43.
- Delacourt, C., Allemand, P., Casson, B. and Vadon, H.** 2004: Velocity field of the ‘La Clapière’ landslide measured by the correlation of aerial and QuickBird satellite images. *Geophysical Research Letters* 31(15), DOI: 10.1029/2004GL020193.
- Dikau, R.** 1989: Application of a digital relief model to landform analysis in geomorphology. In Raper, J., editor, *Three dimensional application in geographic information systems*, London: Taylor and Francis, 51–77.
- Ehlers, M., Gähler, M. and Janowsky, R.** 2003: Automated analysis of ultra high resolution remote sensing data for biotope type mapping: new possibilities and challenges. *ISPRS Journal of Photogrammetry and Remote Sensing* 57, 315–26.
- French, J.R.** 2003: Airborne LiDAR in support of geomorphological and hydraulic modelling. *Earth Surface Processes and Landforms* 28, 321–35.
- Geist, T., Lutz, E. and Stötter, J.** 2003: Airborne laser scanning technology and its potential for applications in glaciology. ISPRS Workshop on 3-D Reconstruction from Airborne Laserscanner and INSAR Data, Dresden.
- Gendrin, A., Mangold, N., Bibring, J.-P., Langevin, Y., Gondet, B., Poulet, F., Bonello, G., Quantin, C., Mustard, J., Arvidson, R. and LeMouëlic, S.** 2005: Sulfates in Martian layered terrains: the OMEGA/Mars express view. *Science* 307(5715), 1587–91.
- Glaßer, C. and Reinartz, P.** 2005: Multitemporal and multispectral remote sensing approach for flood detection in the Elbe-Mulde region 2002. *Acta Hydrochimica et Hydrobiologica* 33, 395–403.
- Glenn, N.F., Streutker, D.R., Chadwick, D.J., Thackray, G.D. and Dorsch, S.J.** 2006: Analysis of LiDAR-derived topographic information for characterizing and differentiating landslide morphology and activity. *Geomorphology* 73, 131–48.
- Gorbunov, A.P., Marchenko, S.S. and Seversky, E.V.** 2004: The thermal environment of blocky mate-

- rials in the mountains of Central Asia. *Permafrost and Periglacial Processes* 15, 95–98.
- Gwinner, K., Hauber E., Hoffmann, H., Scholten F., Jaumann, R., Neukum G., Coltelli, M. and Puglisi, G.** 1999: The HRSC-A experiment on high resolution multispectral imaging and DTM generation at the Aeolian Islands. *Proceedings of the 13th International Conference on Applied Geologic Remote Sensing, Vancouver, Canada*, vol. 1, 560–69.
- Haeberli, W.** 1985: Creep of mountain permafrost: internal structure and flow of Alpine rock glaciers. *Versuchsanstalt für Wasserbau, Hydrologie und Glaziologie der Eidgenössischen Technischen Hochschule Zürich, Mitteilungen* 77, 119.
- Haralick, R.M., Shanmugam, K. and Dinstein, I.** 1973: Textural features for image classification. *IEEE Transactions on Systems, Man and Cybernetics SMC-3* 6, 610–21.
- Hauber, E. and Neukum, G.** 2006: Mars: simply red? *Astronomy and Geophysics* 47(2), 16–24.
- Hauber, E., Slupetzky, H., Jaumann, R., Wewel, F., Gwinner, K., and Neukum, G.** 2000: Digital and automated high resolution stereo mapping of the Sonnblick glacier (Austria) with HRSC-A. *Proceedings of EARSel-SIG-Workshop Land Ice and Snow, Dresden/FRG*, June 16–17, 2000.
- Hauber, E., van Gasselt, S., Ivanov, B., Werner, S., Head, J.W., Neukum, G., Jaumann, R., Greeley, R., Mitchell, K.L. and Müller, P.** 2005: Discovery of a flank caldera and very young glacial activity at Hecates Tholus, Mars. *Nature* 434(7031), 356–61.
- Head, J.W., Neukum, G., Jaumann, R., Hiesinger, H., Hauber, E., Carr, M., Masson, P., Foing, B., Hoffmann, H., Kreslavsky, M., Werner, S., Milkovich, S. and van Gasselt, S.** 2005: Tropical to mid-latitude snow and ice accumulation, flow and glaciation on Mars. *Nature* 434(7031), 346–51.
- Heinzel, V., Waske, B., Braun, M. and Menz, G.** 2005: The potential of multitemporal and multisensorial remote sensing data for the extraction of biophysical parameters of wheat. *Proceedings of SPIE – The International Society for Optical Engineering*, 5976.
- Helbert, J., Reiss, D., Hauber, E. and Benkhoff, J.** 2005: Limits on the burial depth of glacial ice deposits on the flanks of Hecates Tholus, Mars. *Geophysical Research Letters* 32(17), 1–4.
- Hörsch, B.** 2003: *Zusammenhang zwischen Vegetation und Relief in alpinen Einzugsgebieten des Wallis (Schweiz). Ein Multiskaliger GIS- und Fernerkundungsansatz.* Bonner Geographische Abhandlungen 110. Sankt Augustin: Asgard Verlag, 256 pp.
- Huggel, C., Zraggen-Oswald, S., Haeberli, W., Käab, A., Polkvoj, A., Galushkin, I. and Evans, S.G.** 2005: The 2002 rock/ice avalanche at Kolka/Karmadon, Russian Caucasus: assessment of extraordinary avalanche formation and mobility, and application of QuickBird satellite imagery. *Natural Hazards and Earth System Science* 5, 173–87.
- Ivanov, M.A., Korteniemi, J., Kostama, V.-P., Aittola, M., Raitala, J., Glamoclija, M., Marinangeli, L. and Neukum, G.** 2005: Major episodes of the hydrologic history in the region of Hesperian Planum, Mars. *Journal of Geophysical Research E: Planets* 110(12), 1–28.
- Jaumann, R., Reiss, D., Frei, S., Neukum, G., Scholten, F., Gwinner, K., Roatsch, T., Matz, K.-D., Mertens, V., Hauber, E., Hoffmann, H., Köhler, U., Head, J.W., Hiesinger, H. and Carr, M.H.** 2005: Interior channels in Martian valleys: constraints on fluvial erosion by measurements of the Mars Express High Resolution Stereo Camera. *Geophysical Research Letters* 32(16), 1–4.
- Käab, A. and Vollmer, M.** 2000: Surface geometry, thickness changes and flow fields on creeping mountain permafrost: automatic extraction by digital image analysis. *Permafrost and Periglacial Processes* 11, 315–26.
- Käab, A., Frauenfelder, R. and Roer, I.** 2007: On the response of rockglacier creep to surface temperature increase. *Global and Planetary Change*, in press.
- Käab, A., Huggel, C., Fischer, L., Guex, S., Paul, F., Roer, I., Salzmann, N., Schläefli, S., Schmutz, K., Schneider, D., Strozzii, T. and Weidmann, Y.** 2005: Remote sensing of glacier- and permafrost-related hazards in high mountains: an overview. *Natural Hazards and Earth System Science* 5, 527–54.
- Kawamura, M., Tsujino, K. and Tsujiko, Y.** 2003: Analysis of slope failures due to the 2000 Tokai heavy rainfall using high resolution satellite images. *International Geoscience and Remote Sensing Symposium (IGARSS)* 4, 2413–18.
- Kennett, M. and Eiken, T.** 1997: Airborne measurement of glacier surface elevation by scanning laser altimeter. *Annals of Glaciology* 24, 293–96.
- Keramitsoglou, I., Kontoes, C., Koutroumbas, K., Sykioti, O. and Sifakis, N.** 2005: Mapping of forest species and tree density using new Earth Observation sensors for wildfire applications. *Proceedings of SPIE – The International Society for Optical Engineering*, 5976.
- Kimes, D.S., Ranson, K.J., Sun, G. and Blair, J.B.** 2006: Predicting lidar measured forest vertical structure from multi-angle spectral data. *Remote Sensing of Environment* 100, 503–11.
- Kobler, A., Dzeroski, S. and Keramitsoglou, I.** 2006: Habitat mapping using machine learning-extended kernel-based reclassification of an Ikonos satellite image. *Ecological Modelling* 191, 83–95.
- König, O.** 2006: Korngrößenmuster auf Oberflächen alpiner Sedimentspeicher. Thesis, University of Bonn, 130 pp.
- Korteniemi, J., Kostama, V.-P., Törmänen, T., Aittola, M., Ohman, T., Lahtela, H., Raitala, J.**

- and **Neukum, G.** 2005: Complex geology of two large impact craters in Tyrrhena Terra, Mars: detailed analysis using MEX HRSC camera data. *Journal of Geophysical Research E: Planets* 110(12), 1–21.
- Kovanen, D.J.** and **Slaymaker, O.** 2004: Relict shorelines and ice flow patterns of the northern Puget Lowland from lidar data and digital terrain modelling. *Geografiska Annaler, Series A: Physical Geography* 86, 385–400.
- Lane, S.N., Richards, K.S.** and **Chandler, J.H.**, editors 1997: *Landform monitoring, modelling and analysis*. Chichester: Wiley, 440 pp.
- Lane, S.N., Westaway, R.M.** and **Hicks, D.M.** 2003: Estimation of erosion and deposition volumes in a large, gravel-bed, braided river using synoptic remote sensing. *Earth Surface Processes and Landforms* 28, 249–71.
- Lehmann, F., Bucher, T., Hese, S., Hoffmann, A., Mayer, S., Oschuetz, F.** and **Zhang, Y.** 1998: Die Kombination von hyperspektralen HyMap-Daten und HRSC-A Multispektral- und DGM-Daten zur Validierung und Nutzung in verschiedenen Anwendungsgebieten. *Mitteilung – Deutsche Forschungsanstalt fuer Luft- und Raumfahrt* 98, 89–104.
- Leser, C.** 2003: Entwicklung operationell einsetzbarer Methoden zur Biotoptypen-Kartierung anhand hochauflösender HRSC-Daten. Dissertation thesis, Technische Universität Berlin, 159 pp.
- McKean, J.** and **Roering, J.** 2004: Objective landslide detection and surface morphology mapping using high-resolution airborne laser altimetry. *Geomorphology* 57, 331–51.
- Metternicht, G., Hurni, L.** and **Gogu, R.** 2005: Remote sensing of landslides: an analysis of the potential contribution to geo-spatial systems for hazard assessment in mountainous environments. *Remote Sensing of Environment* 98, 284–303.
- Murray, J.B., Muller, J.-P., Neukum, G., Werner, S.C., Van Gasselt, S., Hauber, E., Markiewicz, W.J., Head, J.W. III, Foing, B.H., Page, D., Mitchell, K.L.** and **Portyankina, G.** 2005: Evidence from the Mars Express High Resolution Stereo Camera for a frozen sea close to Mars' equator. *Nature* 434(7031), 352–56.
- Neukum, G.** 2001: The airborne HRSC-AX cameras: evaluation of the technical concept and presentation of application results after one year of operations. *Photogrammetric Week* 01, 117–31.
- Neukum, G., Jaumann, R., Hoffmann, H., Hauber, E., Head, J.W., Basilevsky, A.T., Ivanov, B.A., Werner, S.C., van Gasselt, S., Murray, J.B.** and **McCord, T.** 2004: Recent and episodic volcanic and glacial activity on Mars revealed by the High Resolution Stereo Camera. *Nature* 432, 971–79.
- Nichol, J.** and **Wong, M.S.** 2005: Satellite remote sensing for detailed landslide inventories using change detection and image fusion. *International Journal of Remote Sensing* 26, 1913–26.
- Ni-Meister, W.** 2005: 3D vegetation structure extraction from lidar remote sensing. *Proceedings of SPIE – The International Society for Optical Engineering* 5887, 1–7.
- Nyenhuis, M.** 2005: Permafrost und Sedimenthaushalt in einem alpinen Geosystem. Thesis, Universität Bonn, 214 pp.
- Otto, J.C.** 2007: Paraglacial sediment storage quantification in the Turtmann Valley, Swiss Alps. PhD thesis, University of Bonn. Retrieved 12 february 2007 from http://hss.ulb.uni-bonn.de/diss_online/math_nat_fak/2006/otto_jan_christoph/
- Otto, J.C.** and **Dikau, R.** 2004: Geomorphologic system analysis of a high mountain valley in the Swiss Alps. *Zeitschrift für Geomorphologie* 48, 323–41.
- Perez, F.L.** 1998: Talus fabric, clast morphology, and botanical indicators of slope processes on the Chaos Crags (California Cascades), USA. *Géographie Physique et Quaternaire* 52, 1–22.
- Pike, R.J.** and **Dikau, R.**, editors 1995: Geomorphometry. *Zeitschrift für Geomorphologie*, N.F. Supplement-Band 101.
- Poulet, F., Bibring, J.-P., Mustard, J.F., Gendrin, A., Mangold, N., Langevin, Y., Arvidson, R.E., Gondet, B.** and **Gomez, C.** 2005: Phyllosilicates on Mars and implications for early martian climate. *Nature* 438(7068), 623–27.
- Rasemann, S.** 2004: Geomorphometrische Struktur eines mesoskaligen alpinen Geosystems. *Bonner Geographische Abhandlungen*, Heft 111. Retrieved 16 January 2007 from http://hss.ulb.uni-bonn.de/diss_online/math_nat_fak/2003/rasemann_stefan/index.htm
- Rasemann, S., Schmidt, J., Schrott, L.** and **Dikau, R.** 2004: Geomorphometry in mountain terrain. In Bishop, M. and Shroder, J.F., editors, *Geographic information science in mountain geomorphology*, Heidelberg: Springer, 101–45.
- Reiss, D., Hauber, E., Michael, G., Jaumann, R.** and **Neukum, G.** 2005: Small rampart craters in an equatorial region on Mars: implications for near-surface water or ice. *Geophysical Research Letters* 32(10), 1–4.
- Roer, I., Käab, A.** and **Dikau, R.** 2005a: Rockglacier kinematics derived from small-scale aerial photography and digital airborne pushbroom imagery. *Zeitschrift für Geomorphologie – N.F.* 49, 73–87.
- 2005b: Rockglacier acceleration in the Turtmann valley (Swiss Alps): probable controls. *Norsk Geografisk Tidsskrift – Norwegian Journal of Geography* 59, 157–63.
- Saroli, M., Stramondo, S., Moro, M.** and **Doumaz, F.** 2005: Movements detection of deep seated gravitational slope deformations by means of InSAR data and photogeological interpretation: northern Sicily case study. *Terra Nova* 17, 35–43.
- Schmidt, J.** and **Dikau, R.** 1999: Extracting geomorphometric attributes and objects from digital

- elevation models – semantics, methods, future needs. In Dikau, R. and Saurer, H., editors, *GIS for earth surface systems*, Stuttgart: Gebrüder Borntraeger, 153–74.
- Scholten, F., Gwinner, K. and Wewel, F.** 2002: Angewandte digitale Photogrammetrie mit der HRSC. *Photogrammetrie-Fernerkundung-Geoinformation* 5, 317–32.
- Singh, L.P., van Westen, C.J., Ray, P.K.C. and Pasquali, P.** 2005: Accuracy assessment of InSAR derived input maps for landslide susceptibility analysis: a case study from the Swiss Alps. *Landslides* 2, 221–28.
- Smith, M.J. and Clark, C.D.** 2005: Methods for the visualization of digital elevation models for landform mapping. *Earth Surface Processes and Landforms* 30, 885–900.
- Squarzonzi, C., Delacourt, C. and Allemand, P.** 2003: Nine years of spatial and temporal evolution of the La Valette landslide observed by SAR interferometry. *Engineering Geology* 68, 53–66.
- Staley, D.M., Wasklewicz, T.A. and Blaszczyński, J.S.** 2006: Surficial patterns of debris flow deposition on alluvial fans in Death Valley, CA using airborne laser swath mapping data. *Geomorphology* 74, 152–63.
- Strozzi, T., Kääb, A. and Frauenfelder, R.** 2004: Detecting and quantifying mountain permafrost creep from in situ inventory, space-borne radar interferometry and airborne digital photogrammetry. *International Journal of Remote Sensing* 25, 2919–31.
- Tamburini, A., Deline, P. and Mortara, G.** 2005: Time-space modelling with terrestrial lidar: monitoring ice cliff evolution of the Miage Glacier, Italy, with ILRIS-3D. *GIM International* 19(11), 31–33.
- Toutin, T.** 2004: Comparison of stereo-extracted DTM from different high-resolution sensors: SPOT-5, EROS-A, IKONOS-II, and QuickBird. *IEEE Transactions on Geoscience and Remote Sensing* 42, 2121–29.
- Voß, K.** 2004: Remote sensing and landscape metrics to identify and to assess site-specific damage in cultivation systems of Central Europe. *Erdkunde* 58, 283–89.
- Wewel, F., Scholten, F. and Gwinner, K.** 2000: High Resolution Stereo Camera (HRSC) – multispectral 3D-data acquisition and photogrammetry data processing. *Canadian Journal of Remote Sensing* 26, 466–74.
- Xu, K., Zhang, J., Watanabe, M. and Sun, C.** 2004: Estimating river discharge from very high-resolution satellite data: a case study in the Yangtze River, China. *Hydrological Processes* 18, 1927–39.
- Yang, C., Everitt, J.H. and Bradford, J.M.** 2004: Using high resolution QuickBird satellite imagery for cotton yield estimation. *ASAE Annual International Meeting*, 893–904.
- Yoshikawa, K. and Hinzman, L.D.** 2003: Shrinking thermokarst ponds and groundwater dynamics in discontinuous permafrost near Council, Alaska. *Permafrost and Periglacial Processes* 14, 151–60.
- Zhang, C.P., Niu, J.M., Dong, J.J. and Li, M.** 2006a: Vegetation mapping and spatial pattern analysis using IKONOS data: a case study in the Wufendigou area. *Acta Ecologica Sinica* 26, 449–56.
- Zhang, J.H., Wang, K., Bailey, J.S. and Wang, R.C.** 2006b: Predicting nitrogen status of rice using multispectral data at canopy scale. *Pedosphere* 16, 108–17.